



Published in final edited form as:

SoftwareX. 2023 July ; 23: . doi:10.1016/j.softx.2023.101482.

McDAPS: A multi-channel physiological signals display and analysis system for clinical researchers

Wanwara Thuptimjang^{a,*}, Patjanaporn Chalacheva^b, Thomas D. Coates^c, Michael C.K. Khoo^d

^aInstitute of Biomedical Engineering, Department of Biomedical Sciences and Biomedical Engineering, Faculty of Medicine, Prince of Songkla University, Hat Yai, Songkhla, Thailand

^bBiomedical Engineering Department, Carnegie Mellon University, Pittsburgh, PA, United States of America

^cHematology Section, Cancer and Blood Disease Institute, Children's Hospital Los Angeles, University of Southern California Keck School of Medicine, Los Angeles, CA, United States of America

^dDepartment of Biomedical Engineering, University of Southern California, Los Angeles, United States of America

Abstract

We introduce McDAPS, an interactive software for assessing autonomic imbalance from non-invasive multi-channel physiological recordings. McDAPS provides a graphical user interface for data visualization, beat-to-beat processing and interactive analyses. The software extracts beat-to-beat RR interval systolic blood pressure, diastolic blood pressure, the pulse amplitude of photoplethysmogram and the pulse-to-pulse interval. The analysis modules include stationary and time-varying power spectral analyses, moving-correlation analysis and univariate analyses. Analyses can also be performed in batch mode if multiple datasets have to be processed in the same way. The program exports results in standard CSV format.

McDAPS runs in MATLAB, and is supported on MS Windows and MAC OS systems. The MATLAB source code is available at <https://github.com/thuptimd/McDAPS.git>.

Keywords

ANS; Beat-to-beat; Power spectral analysis; Cross correlation

This is an open access article under the CC BY-NC-ND license (<http://creativecommons.org/licenses/by-nc-nd/4.0/>).

*Corresponding author. wanwara.t@psu.ac.th (Wanwara Thuptimjang).

Appendix A. Supplementary data

Supplementary material related to this article can be found online at <https://doi.org/10.1016/j.softx.2023.101482>.

Declaration of competing interest

The authors declare that they have no known competing financial interests or personal relationships that could have appeared to influence the work reported in this paper.

Code metadata	
Current code version	v2.0
Permanent link to code/repository used for this code version	https://github.com/ElsevierSoftwareX/SOFTX-D-23-00242
Permanent link to reproducible capsule	'none'
Legal code license	GNU General Public License v3.0
Code versioning system used	git
Software code languages, tools and services used	MATLAB 2022a
Compilation requirements, operating environments and dependencies	MS windows, MAC OS systems MATLAB, Signal Processing Toolbox, Image Processing Toolbox, Statistics and Machine Learning Toolbox
If available, link to developer documentation/manual	https://github.com/thuptimd/McDAPS/blob/840f2e0454028a65650ee1e971c292b9d5e069dc/Manual/McDAPs_manual_v2.0.pdf
Support email for questions	wanwara.t@psu.ac.th

1. Motivation and significance

The autonomic nervous system (ANS) is divided into two divisions — the sympathetic (SNS) and the parasympathetic nervous system (PNS). The imbalance between these two divisions, specifically when the SNS is hyperactive, may interrupt complex interactions among several physiologic mechanisms that act to maintain physiological parameters such as cardiac output, heart rate or blood pressure within normal limits. In many cohort studies, it has been shown that autonomic imbalance is a significant indicator of overall health and associated with worsening conditions of several diseases such as hypertension [1], chronic heart failure [2,3], metabolic syndrome [4], diabetes [5–7] and obstructive sleep apnea [8].

In laboratory setting, it is common to assess autonomic function in human subjects by having a participant perform physical maneuver or mental tasks [9] while autonomic-mediated physiological responses are recorded. The most important autonomic markers, such as the statistical features or the frequency power of the R-to-R interval (RRI) of the electrocardiogram (ECG), indicate the overall balance of cardiac autonomic activity [10–12]. Other autonomic markers, such as the frequency power of beat-to-beat blood pressure (BP) variability or photoplethysmographic pulse wave (PPG) variability, indicate sympathetic and local modulation of vasomotor activity [13–18]. More complex markers, such as cardiac baroreflex sensitivity [19,20], involve adjusting heart rate variability with blood pressure variability.

Most available packages to assess autonomic imbalance such as Kubios [21], HRVanalysis [22], gHRV [23], Kardia [24] primarily focus on utilizing one signal, especially RRI to analyze heart rate variability. This is impractical for modern experimental settings that adopt a multi-modality platform to aggregate data such as AcqKnowledge (Biopac, Inc.) and LabChart (ADInstruments). To the best of our knowledge, only a few toolboxes are available to analyze other physiological recordings such as BP or PPG. The examples are ANSlab

[25], PhysioNet Cardiovascular Signal Toolbox (PCST) [26] and pyphysio [27]. However, only a commercialized version of ANSLab provides beat-to-beat processing for ECG, BP and PPG. PCST and pyphysio do not provide a graphical user interface and are designed for creating custom processing pipelines that require users to write programs for data analysis. Most of the available programs also lack sophisticated tools to define, select or save multiple segments for analyses. Moreover, results are not exported in a format that can be easily transferred to standard statistical packages for further analyses with clinical data.

Herein, we introduce McDAPS, an alternative software to evaluate autonomic imbalance from noninvasive physiological recordings. McDAPS was developed with the goal of assessing autonomic regulation through the visualization and analysis of respiratory and cardiovascular signals, in addition to ECG, that are commonly monitored in the clinical environment. The software provides basic signal operations, beat-to-beat processing as well as stationary power spectral analysis, time-varying power spectral analysis, moving correlation analysis and descriptive statistics. The user can visually define, select, and analyze multiple segments from multiple signals using a batch processing option. The package outputs derived parameters as well as subject identification variables in a format that can be imported into standard statistical packages.

2. Software description

2.1. Software architecture

McDAPS is developed using a UI design environment of MATLAB known as GUIDE. McDAPS is comprised of six sub-modules specifically built for three different purposes — (1) data visualization (2) beat-to-beat preprocessing and (3) analyses.

All the modules are treated as separated components because they interact with the data and display results differently. Thus, each module is represented by one MATLAB figure file (Fig-file), and one MATLAB script file (M-file) associated with the graphic components. For example, the main module is represented by `main_DataBrowser.fig` and `main_DataBrowser.m`.

`main_DataBrowser.fig` and `main_DataBrowser.m` are located in a top-level folder, while the rest of the Fig-files and M-files are stored in sub-folders. To use our software package, the user can simply add the folder of McDAPS to MATLAB search path, then run `main_DataBrowser.m`.

2.2. Software functionalities

For ease of use, the user accesses all the modules via the main module called “Data Browser”. In Data Browser, the user imports data as a MATLAB-binary file (MAT-file), and can visualize signals up to thirteen plots. Its main function is to help the user visually inspect the patterns in physiological signals induced by autonomic stimuli. Using the Data Browser’s toolkit, the user labels the analysis regions as “tags” for analysis with other modules.

In a typical analysis workflow, the user may need to extract beat-to-beat signals from raw measurements via the beat-to-beat module before defining tags. After preprocessing, the user can access the analysis modules to perform power spectral analysis, moving correlation or calculate descriptive statistics.

2.2.1. The main module: Data browser—Fig. 1. shows a screenshot of Data Browser after importing a MAT-file containing raw measurements and processed beat-to-beat signals from a single subject participating in the heat-pain study [28]. This example specifically involves the selection and plotting of the pain stimulus (therm), PPG and the pulse amplitude of a photoplethysmogram (PPG_a) using the visualization tool (Fig. 1(a), (b)). The reduction in PPG_a during the pain stimulus (“Pain” tag) indicated a decrease in microvascular blood flow. Users can save the plotted signals and their order as a plot template (.MAT). They have control over window size, plot order, line color, and style. Users can zoom, retrieve data point values, pan axes view, and use “Jump” to navigate to specific time points. Data transformations like normalization, scaling, and shifting are also available.

The tagging feature of Data Browser offers the most functionality. The user can draw regions on the plotted signal to create tags (Fig. 1(c)). When a tag is created, another row appears on the tag table (Fig. 1(d)). The row has the tag’s name, the start position, the end position, its duration, the signal and the MATfile from which the tag was created. Tags can be exported into a comma-separated (CSV) file (Fig. 1(e), Fig S1). These tags can then be used to restrict analysis in other signals to the same time region and can be accessed in batch processing of multiple data files.

Events during an experiment, such as application of a stimulus can be marked and stored with the data file (Fig. 1(f)). When the user imports a MAT-file with event marks, they appear on the event table. The user can click on the event table to locate the time the event occurs on the plots.

2.2.2. The beat-to-beat module (B2B)—B2B (Fig. 2.) provides three processing options to extract beat-to-beat values of ECG, BP and PPG. The beat-to-beat values available on McDAPS are RRI, systolic blood pressure (SBP), diastolic blood pressure (DBP), mean arterial pressure (MAP), the pulse-to-pulse interval (PPI) and PPG_a.

B2B, detects the R-peaks from the ECG using an in-house adaptive thresholding algorithm. The R-peak is the maximum point which exceeds the 90th percentile value of the ECG in 1.5-second window. Once the first R-peak in the ECG is identified, a new threshold is determined from the next 1.5-second window beginning from the most recently identified R-peak. The process repeats until the end of the signal.

The systolic peaks of BP and PPG are detected using a published algorithm [29]. The detected systolic peaks are then used to search for the corresponding troughs. For BP processing, the systolic peak and the trough are SBP and DBP respectively. MAP is calculated as the sum of 2/3 DBP and 1/3 SBP.

While the processing is automatic, users can correct the algorithm detection via Add/Reject buttons. B2B exports the interpolated beat-to-beat time-series that is uniformly sampled at 2 Hz [30] to Data Browser.

2.2.3. Power spectral modules—Stationary power spectral density (Stationary PSD) and time-varying power spectral density (Time-varying PSD) modules (Fig. 3.) compute power spectrum of a signal within the selected tag.

By default, stationary PSD calculates total power, low-frequency power (LF; 0.04–0.15 Hz) and high-frequency power (HF; 0.15–0.4 Hz) of the selected data segments (e.g. Fig. 3. “pain” tag). However, the user can modify the frequency ranges, frequency resolution and detrending order in the module’s setting. Stationary PSD displays the power spectra and exports the results into a CSV file.

Time-varying PSD applies the stationary PSD analysis to a sliding 60 s window that is moved along the signal one sample at a time. For each sliding step, LF and HF are derived from the calculated PSD. The outputs of this analysis are the time-series of LF and HF of the signal under investigation. The outputs are exported to Data Browser.

The PSD can be estimated using Welch’s method [31], an autoregressive (AR) model [32] or an input-adjusted autoregressive model [33,34]. The PSD estimate from Welch’s method is the average of periodograms obtained from the overlapping and windowed data segments. The AR method assumes that the signal can be modeled as the output of an AR filter (regressed on its own past values) driven by white noise, where the AR filter coefficients are estimated and optimized using the Akaike information criterion [35]. The PSD estimate can then be obtained by taking the Fourier transform of the optimized AR filter. The input-adjusted autoregressive method is an extension of the AR method and is used when the influence of a correlating factor (a time-varying input, most commonly respiration) needs to be attenuated. This method was originally developed to correct for the influence of non-uniform ventilatory patterns on heart rate variability [33,34] — i.e. it would produce an estimate what the heart rate variability index would be under tidal breathing conditions with the same ventilation.

2.2.4. Moving correlation module (MC)—MC detects similarity between two signals within the selected tag by cross-correlation analysis (Fig. 4). The analysis yields the Pearson and Spearman correlation coefficients and the time lag between two signals where the strongest correlation occurs. The maximum correlation was determined from the start of the analysis tag to 10 s after (based on the defined search window. The follow-up significance test is used to statistically distinguish the pattern identified as a response from the pattern that may arise simply from spontaneous fluctuations in the signal that coincide with the stimulus [36]. The outputs of the module are shown in the result table and can be saved as a CSV file.

2.2.5. Feature extraction module (FEX)—FEX computes descriptive statistics, e.g. mean, median, min, max, coefficient of variation, as well as fits a curve (exponential, polynomial and sigmoid) of the data within the selected tags.

2.2.6. Batch analyses—In clinical research, the same analysis of physiological signals may be performed on multiple subjects with difference characteristics. Batch analyses (Fig. 5.) simplify this process by allowing each analysis module to run on the directory of MAT-files to output analysis within pre-defined tags. Fig. 6. displays the outputs of batch processing performed in Stationary PSD module. In each data-file, two signals – RRI and SBP were analyzed within two tagged regions – Extbaseline1 and Task1. Each calculated parameter was output as a row. The “operation tag” is the name of the output variables particular to the analysis module (“operation”). The number of rows per analysis can vary depending on the output of the particular analysis module (see Fig S2. for the batch analysis output of moving-correlation analysis); however, the number of columns is always the same. Thus, all of the analyses for all of the subjects can be concatenated into one file for loading into the statistical software. As the subject ID is carried in every row of the output, the investigator can join this result table with a separate file that contains the subject ID and clinical data like diagnosis, gender, age etc. This approach allows modification and addition of the analysis modules without having to change the output format.

3. Illustrative examples

In this section, we illustrate how the software is used to analyze autonomic changes in response to heat-pain pulses applied to the forearm [28,36]. In this experiment, the magnitude of the heat-pain stimuli was measured as changes in voltage which is negatively proportional to changes in skin temperature induced by the thermal pain device (TSI-II).

In the first example (Fig. 4.), we were interested to see if decreases in microvascular blood flow measured by PPGa (Fig. 4: 2nd panel) were associated with the thermal pattern (Fig. 4; 1st signal). We performed cross-correlation between the thermal pain signal and PPGa to determine if the pattern of pain stimuli was present in the blood flow response. Using the moving correlation module, we cross-correlated “therm” and “ppga” during the pain pulses labeled as “Pain Tag”.

The table entries in Fig. 4. include the identified maximum correlation coefficients (Pearson and Spearman) and the time lag between ‘therm’ and ‘ppga’ where the maximum correlation occurs. The third and fourth panels of Fig. 4. display the Pearson and Spearman cumulative distribution functions constructed from correlation coefficients between “therm” (in the test region) and “ppga” in all possible sections of the baseline region. The vertical line indicates where the maximum correlation during pain is relative to the baseline “null” distribution. In this subject, the maximum correlation locates to the far left of the cumulative null distribution function. This indicates that the pattern observed in the peripheral blood flow during pain application is caused by pain rather than by random fluctuations in the peripheral blood flow.

In the second example (Fig. 3.), we present an example of heart rate variability analysis (HRV) using the Stationary PSD. We applied Welch method to calculate power spectra of sections of the RRI signal during the pain pulses marked by the PAIN tag indicated in red in the left panel of Fig. 3. The left section of the browser screen (Fig. 3.) shows the options for the PSD module analysis, including the signal of interest, in this case “rri”, and the tagged

section of the signal to be analyzed, in this case “Pain”. The right panel displays the power spectrum of HRV calculated within the “Pain” tag. This run produced one row in the result table for the total power, and one for HF and LF. The output parameters were concatenated to the parameters produced by the previous calculation on the “Extbaseline1” tag.

In this particular subject, we found that the total power dropped during the pain stimulus, suggesting that the overall HRV decreased. In addition, both LF and HF decreased during the stimulus, indicating that the reduction in HRV was from parasympathetic withdrawal.

4. Impact

The ANS alterations not only heighten the risk of cardiovascular mortality but may also worsen other complications as disease progresses [37,38]. Therefore, understanding the role of ANS dysfunction in the pathophysiology of diseases may be helpful in (1) making diagnosis of diseases in early stages (2) stratifying risk among patients and (3) preventing adverse outcomes.

In research setting, autonomic assessment is commonly carried out by stimulating cardiovascular responses with stressors such as head-up tilt, isometric hand grip test or mental arithmetic [9]. McDAPS provides a valuable tool to process beat-to-beat cardiovascular signals and inspect deviations in the signals by means of power calculations, moving correlation and descriptive statistics.

With its interface, users can easily define analysis regions directly from the plots to evaluate how autonomic biomarkers, change from one condition to another. Computation can be performed in batch. Results are exported into a CSV file and organized in a long format such that autonomic biomarkers are listed based on analysis regions, signals and data-files to support further statistical analysis.

McDAPS has been used with our previous work to derive physiological biomarkers that represent autonomic control of the heart and microvascular blood flow associated with heat-pain, cold-pain and mental stress vasoconstriction responses in sickle cell disease patients and healthy subjects [39–41].

5. Conclusion

We have developed a software package for assessing autonomic imbalance. The software is geared towards users with little to no technical/programming background. While other available non-commercial software packages are dedicated to specific types of analysis, e.g. heart rate variability, we offer a versatile tool set that can be applied to any set of multiple physiological signals. The package offers batch analyses that allow the user to replicate the same set of analysis procedures on multiple data files in one session. The output format of the analysis results can readily be imported by statistical software and easily be linked to clinical information related to the study subjects.

Supplementary Material

Refer to Web version on PubMed Central for supplementary material.

Acknowledgments

This work was supported by National Institutes of Health National Heart, Lung and Blood Institute, United States of America, grant U01 HL117718. We thank Payal Shah, Maha Khaleel, Saranya Veluswamy, Christopher Denton, John Sunwoo and Kelby Knox for their helpful feedback and for assistance in the testing process of the software.

Data availability

No data was used for the research described in the article.

References

- [1]. Brook RD, Julius S. Autonomic imbalance, hypertension, and cardiovascular risk. *Am J Hypertens* 2000;13(S4):112S–22S. [PubMed: 10921530]
- [2]. Floras JS. Sympathetic nervous system activation in human heart failure: clinical implications of an updated model. *J Am College Cardiol* 2009;54(5):375–85.
- [3]. Kishi T Heart failure as an autonomic nervous system dysfunction. *J Cardiol* 2012;59(2):117–22. [PubMed: 22341431]
- [4]. Tentolouris N, Argyrakopoulou G, Katsilambros N. Perturbed autonomic nervous system function in metabolic syndrome. *Neuromol med* 2008;10:169–78.
- [5]. Dimitropoulos G, Tahrani AA, Stevens MJ. Cardiac autonomic neuropathy in patients with diabetes mellitus. *World J Diabetes* 2014;5(1):17. [PubMed: 24567799]
- [6]. Pop-Busui R Cardiac autonomic neuropathy in diabetes: a clinical perspective. *Diabetes care* 2010;33(2):434–41. [PubMed: 20103559]
- [7]. Vinik AI, et al. Cardiac autonomic neuropathy in diabetes: a predictor of cardiometabolic events. *Front Neurosci* 2018;12:591. [PubMed: 30210276]
- [8]. Lombardi C, Pengo M, Parati G. Obstructive sleep apnea syndrome and autonomic dysfunction. *Auton Neurosci* 2019;221:102563.
- [9]. Zygmunt A, Stanczyk J. Methods of evaluation of autonomic nervous system function. *Arch Med Sci* 2010;6(1):11–8. [PubMed: 22371714]
- [10]. Sztajzel J Heart rate variability: a noninvasive electrocardiographic method to measure the autonomic nervous system. *Swiss Med Week* 2004;134(35–36):514–22.
- [11]. Shaffer F, Ginsberg JP. An overview of heart rate variability metrics and norms. *Front Public Health* 2017;258. [PubMed: 29034226]
- [12]. Camm AJ, Malik M, Bigger M, Breithardt G, Cerutti S, Cohen RJ, et al. Heart rate variability: standards of measurement, physiological interpretation, and clinical use. *Circulation* 1996;93(5):1043–65. [PubMed: 8598068]
- [13]. Photoplethysmography Allen J. and its application in clinical physiological measurement. *Physiol Meas* 2007;28(3):R1. [PubMed: 17322588]
- [14]. Allen J, Chen F. Low-frequency variability in photoplethysmography and autonomic function assessment. In: *Photoplethysmography*. Elsevier; 2022, p. 277–318.
- [15]. Mizeva I, et al. Quantifying the correlation between photoplethysmography and laser Doppler flowmetry microvascular low-frequency oscillations. *J Biomed Opt* 2015;20(3):037007.
- [16]. Khanoka B, et al. Sympathetically induced spontaneous fluctuations of the photoplethysmographic signal. *Med Biol Eng Comput* 2004;42(1):80–5. [PubMed: 14977226]
- [17]. Pagani M, et al. Extracting autonomic information from oscillations in MSNA. *J Physiol* 2012;590(Pt 3):647. [PubMed: 22298902]

- [18]. Ryan KL, et al. Arterial pressure oscillations are not associated with muscle sympathetic nerve activity in individuals exposed to central hypovolaemia. *J Physiol* 2011;589(21):5311–22. [PubMed: 21930599]
- [19]. Borgers AJ, et al. Determinants of vascular and cardiac baroreflex sensitivity values in a random population sample. *Med Biol Eng Comput* 2014;52(1):65–73. [PubMed: 24142561]
- [20]. Porta A, et al. Peripheral resistance baroreflex during incremental bicycle ergometer exercise: characterization and correlation with cardiac baroreflex. *Front Physiol* 2018;9:688. [PubMed: 29922179]
- [21]. Tarvainen MP, et al. Kubios HRV–heart rate variability analysis software. *Comput Methods Programs Biomed* 2014;113(1):210–20. [PubMed: 24054542]
- [22]. Pichot V, et al. HRVanalysis: a free software for analyzing cardiac autonomic activity. *Front Physiol* 2016;7:557. [PubMed: 27920726]
- [23]. Rodríguez-Liñares L, et al. gHRV: Heart rate variability analysis made easy. *Comput Methods Programs Biomed* 2014;116(1):26–38. [PubMed: 24854108]
- [24]. Perakakis P, et al. KARDIA: A Matlab software for the analysis of cardiac interbeat intervals. *Comput Methods Programs Biomed* 2010;98(1):83–9. [PubMed: 19896748]
- [25]. Blechert J, et al. ANSLAB: Integrated multichannel peripheral biosignal processing in psychophysiological science. *Behav Res Methods* 2016;48:1528–45. [PubMed: 26511369]
- [26]. Goldberger AL, et al. PhysioBank, PhysioToolkit, and PhysioNet: Components of a new research resource for complex physiologic signals. *Circulation* 2000;101(23):e215–20. [PubMed: 10851218]
- [27]. Bizzego A, et al. Pyphysio: A physiological signal processing library for data science approaches in physiology. *SoftwareX* 2019;10:100287.
- [28]. Khaleel M, et al. Individuals with sickle cell disease have a significantly greater vasoconstriction response to thermal pain than controls and have significant vasoconstriction in response to anticipation of pain. *Am J Hematol* 2017;92(11):1137–45. [PubMed: 28707371]
- [29]. Kavsaolu AR, Polat K, Bozkurt MR. An innovative peak detection algorithm for photoplethysmography signals: an adaptive segmentation method. *Turk J Electr Eng Comput Sci* 2016;24(3):1782–96.
- [30]. Berger RD, et al. An efficient algorithm for spectral analysis of heart rate variability. *IEEE Trans Biomed Eng* 1986;(9):900–4. [PubMed: 3759126]
- [31]. Welch P The use of fast Fourier transform for the estimation of power spectra: a method based on time averaging over short, modified periodograms. *IEEE Trans Audio Electroacoust* 1967;15(2):70–3.
- [32]. Shiavi R Introduction to applied statistical signal analysis: guide to biomedical and electrical engineering applications. Elsevier; 2010.
- [33]. Khoo MC, Kim TS, Berry RB. Spectral indices of cardiac autonomic function in obstructive sleep apnea. *Sleep* 1999;22(4):443–51. [PubMed: 10389220]
- [34]. Sangkatumvong S, Coates T, Khoo M. Abnormal autonomic cardiac response to transient hypoxia in sickle cell anemia. *Physiol Meas* 2008;29(5):655. [PubMed: 18460753]
- [35]. Akaike H Information theory and an extension of the maximum likelihood principle. In: Selected papers of Hirotugu Akaike. Springer; 1998, p. 199–213.
- [36]. Sunwoo J, et al. A novel cross-correlation methodology for assessing biophysical responses associated with pain. *J Pain Res* 2018;11:2207. [PubMed: 30323655]
- [37]. May O, Arildsen H. Long-term predictive power of heart rate variability on all-cause mortality in the diabetic population. *Acta Diabetologica* 2011;48:55–9. [PubMed: 20844904]
- [38]. Wulsin LR, et al. Autonomic imbalance as a predictor of metabolic risks, cardiovascular disease, diabetes, and mortality. *J Clin Endocrinol Metabol* 2015;100(6):2443–8.
- [39]. Chalacheva P, et al. Biophysical markers of the peripheral vasoconstriction response to pain in sickle cell disease. *PLoS One* 2017;12(5):e0178353.
- [40]. Shah P, et al. Mental stress causes vasoconstriction in subjects with sickle cell disease and in normal controls. *Haematologica* 2020;105(1):83–90. [PubMed: 30975906]

- [41]. Veluswamy S, et al. Progressive vasoconstriction with sequential thermal stimulation indicates vascular dysautonomia in sickle cell disease. *Blood* 2020.

Author Manuscript

Author Manuscript

Author Manuscript

Author Manuscript

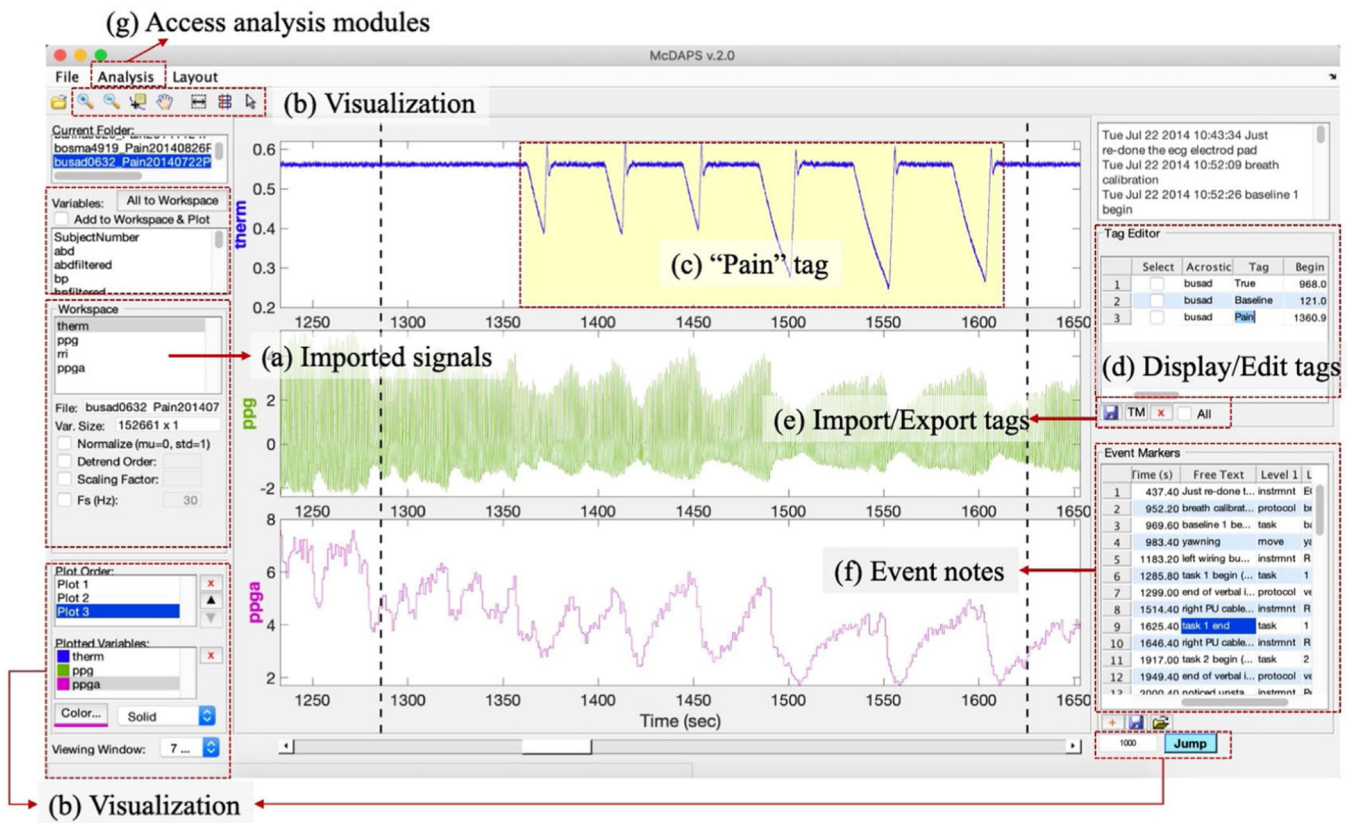


Fig. 1. A snapshot of Data Browser visualizes the signals from the same experiment: (1) heat stimulus, (2) raw PPG, (3) beat-to-beat PPGa.

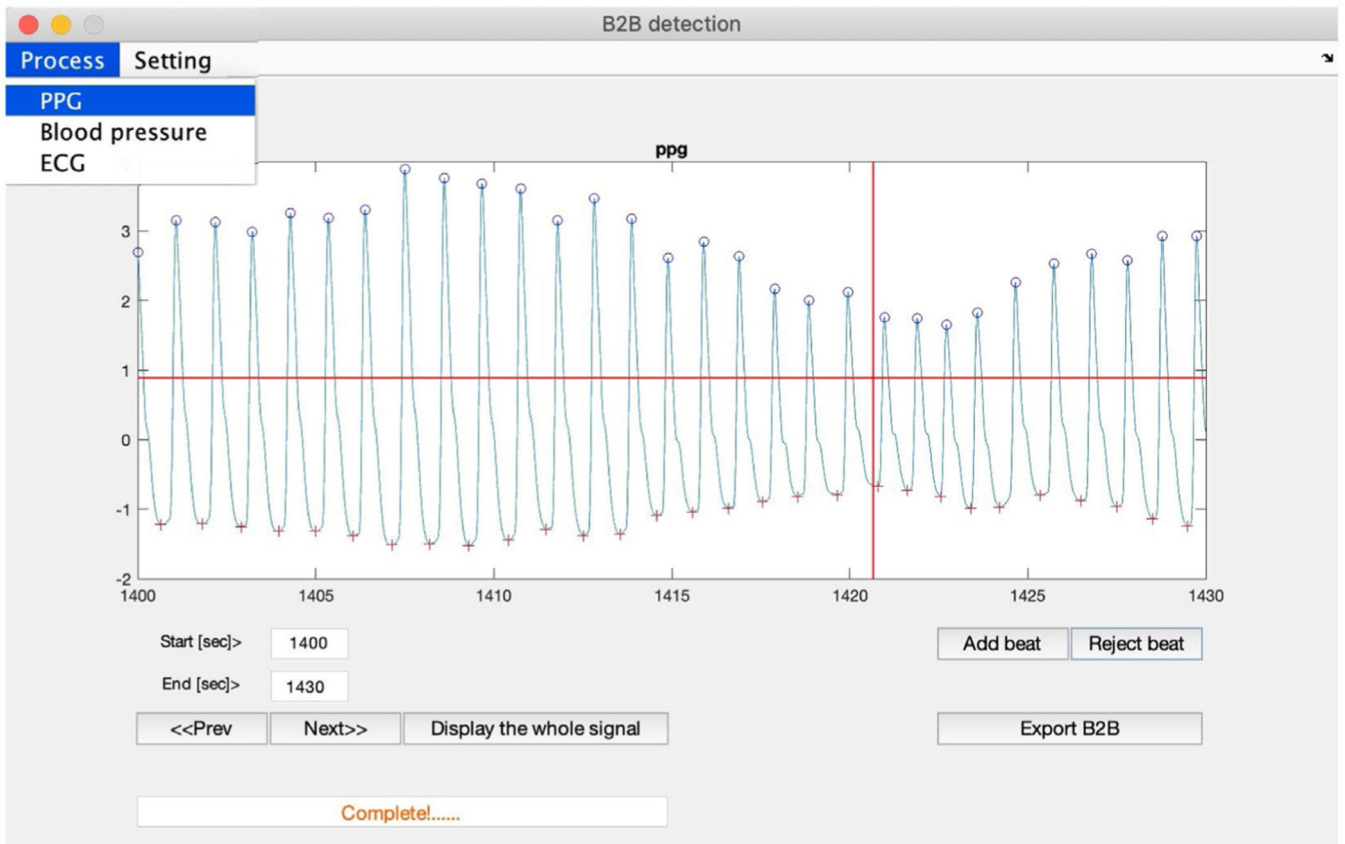


Fig. 2.

A snapshot of the B2B module. The user can adjust the processing window, add and reject incorrect beat detection. The beat-to-beat signals are exported to the main module.

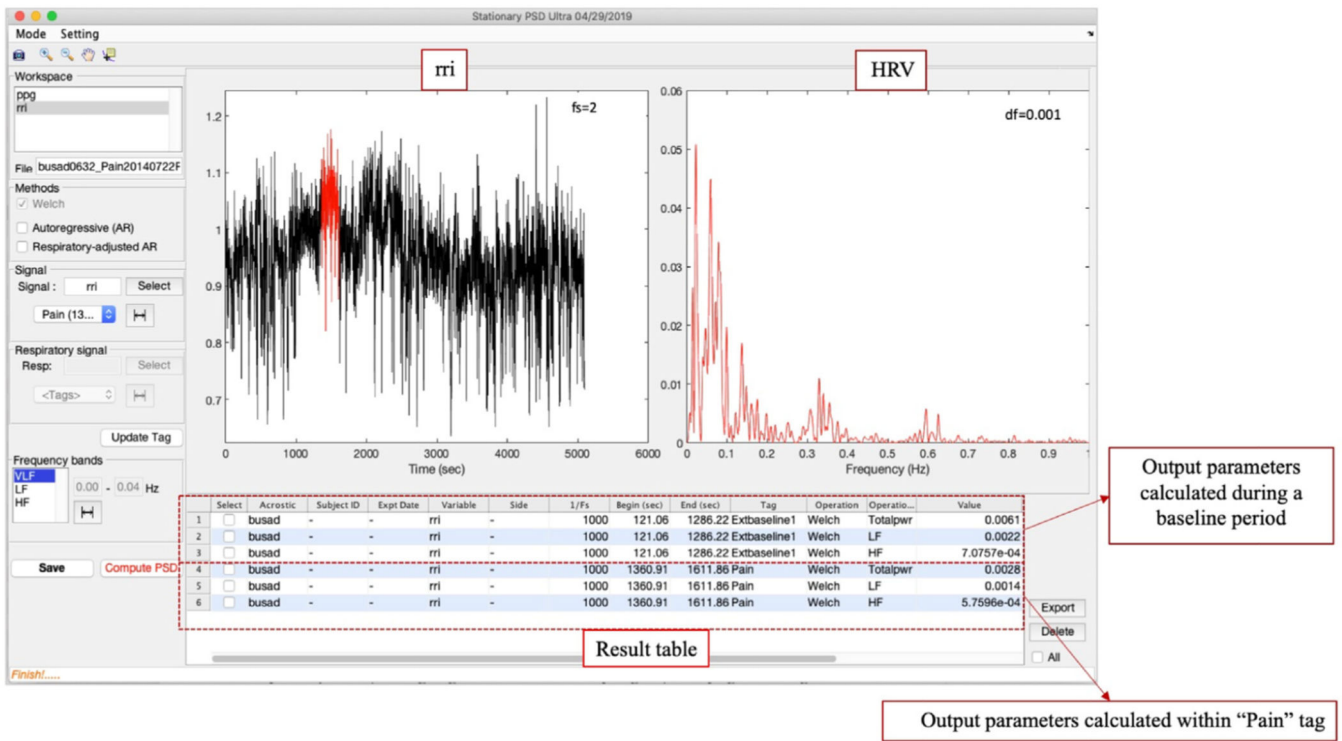


Fig. 3. Example of heart rate variability analysis over the painful stimulus of one healthy subject.

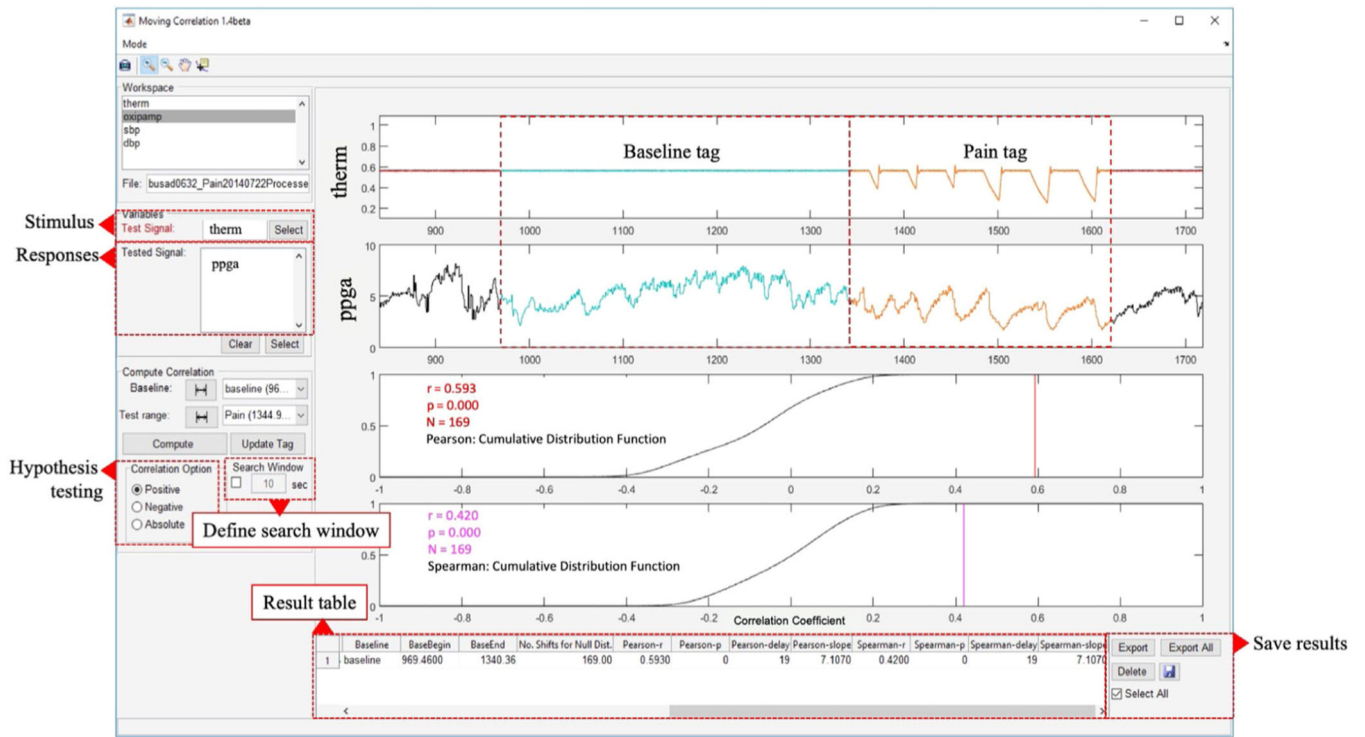


Fig. 4. Application of the moving correlation module to test the significance of blood flow pattern induced by pain pulses.

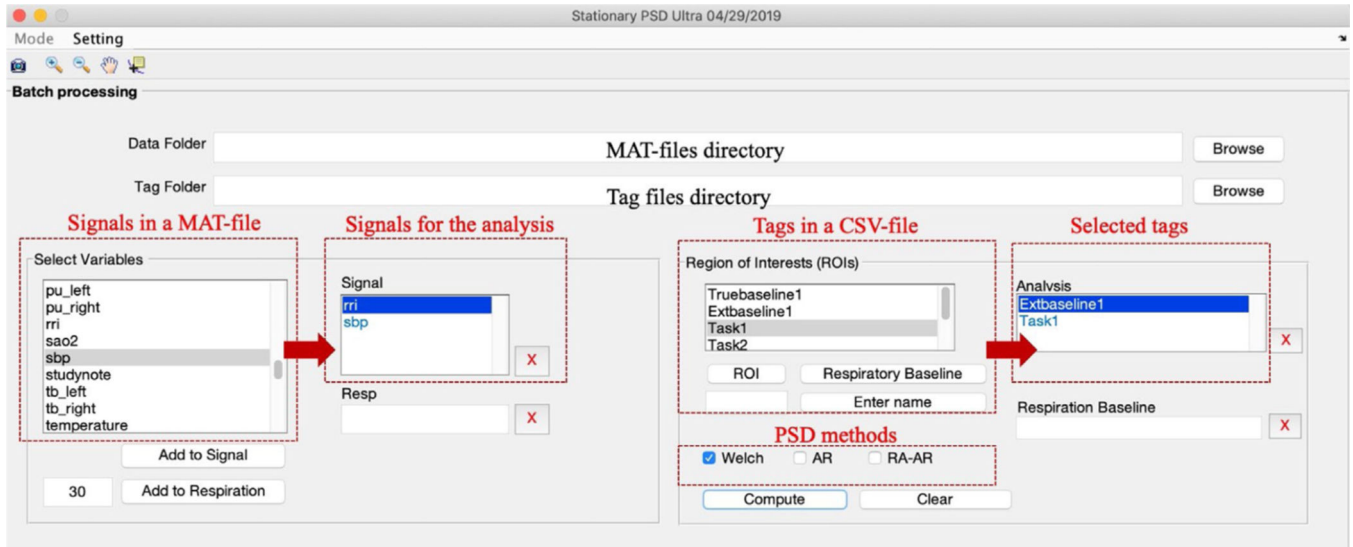


Fig. 5. The interface of batch mode operation of Stationary PSD. “Task1” tag indicated the duration where a specific pattern of heat-pain pulses was given to a subject. “Extbaseline1” tag indicated the baseline period.

MAT-files				Signals		Tags for the analysis		Results	
Acrostic	SubjectID	ExptDate	ExptTime	Variable	CSV	Tag	Operation	OperationTag	Value
A	B	C	D	E	F	G	H	I	J
capbr	1786	20140711	-	rri	Capbr20140711.csv	Extbaseline1	Welch	VLF	0.000517488
capbr	1786	20140711	-	rri	Capbr20140711.csv	Extbaseline1	Welch	LF	0.00100103
capbr	1786	20140711	-	rri	Capbr20140711.csv	Extbaseline1	Welch	HF	0.001655009
capbr	1786	20140711	-	rri	Capbr20140711.csv	Extbaseline1	Welch	TotalPwr	0.003871572
capbr	1786	20140711	-	rri	Capbr20140711.csv	Task1	Welch	VLF	0.000369318
capbr	1786	20140711	-	rri	Capbr20140711.csv	Task1	Welch	LF	0.000548154
capbr	1786	20140711	-	rri	Capbr20140711.csv	Task1	Welch	HF	0.000746853
capbr	1786	20140711	-	rri	Capbr20140711.csv	Task1	Welch	TotalPwr	0.001846563
cores	3016	20140702	-	rri	Cores20140702.csv	Extbaseline1	Welch	VLF	0.000763096
cores	3016	20140702	-	rri	Cores20140702.csv	Extbaseline1	Welch	LF	0.000424744
cores	3016	20140702	-	rri	Cores20140702.csv	Extbaseline1	Welch	HF	0.000310957
cores	3016	20140702	-	rri	Cores20140702.csv	Extbaseline1	Welch	TotalPwr	0.001861269
cores	3016	20140702	-	rri	Cores20140702.csv	Task1	Welch	VLF	0.000489021
cores	3016	20140702	-	rri	Cores20140702.csv	Task1	Welch	LF	0.000260387
cores	3016	20140702	-	rri	Cores20140702.csv	Task1	Welch	HF	0.000261057
cores	3016	20140702	-	rri	Cores20140702.csv	Task1	Welch	TotalPwr	0.001079776
ashja	28914	20140811	-	sbp	Ashja20140811.csv	Extbaseline1	Welch	VLF	6.26438106
ashja	28914	20140811	-	sbp	Ashja20140811.csv	Extbaseline1	Welch	LF	2.236825958
ashja	28914	20140811	-	sbp	Ashja20140811.csv	Extbaseline1	Welch	HF	0.777332338
ashja	28914	20140811	-	sbp	Ashja20140811.csv	Extbaseline1	Welch	TotalPwr	15.10153678
ashja	28914	20140811	-	sbp	Ashja20140811.csv	Task1	Welch	VLF	5.442444158

Fig. 6. The outputs of batch processing performed in Stationary PSD. RRI and SBP were analyzed. The parameters of RRI were shown in row 50–65. Then the parameters of SBP were shown in row 66–70.